Metabolic Adaptation of Airway Smooth Muscle Cells to an SPHK2 Substrate Precedes Cytostasis

Blais-Lecours, Pascale; Laouafa, Sofien; Arias-Reyes, Christian; Santos, Webster L.; Joseph, Vincent; Burgess, Janette K.; Halayko, Andrew J.; Soliz, Jorge; Marsolais, David

Published in:
American Journal of Respiratory Cell and Molecular Biology

DOI:
10.1165/rcmb.2018-0397OC

Publication date:
2020

AJRCMB Articles in Press. Published on 27-June-2019 as 10.1165/rcmb.2018-0397OC

Metabolic adaptation of airway smooth muscle cells to a SPHK2 substrate precedes cytostasis

Authors
Pascale Blais-Lecours[1], Sofien Laouafa[1], Christian Arias-Reyes[1], Webster L. Santos[2], Vincent Joseph[1,3], Janette K. Burgess[4,5], Andrew J. Halayko[6,7], Jorge Soliz[1,3] and David Marsolais[1,3]

Affiliations
1. Centre de recherche de l'Institut Universitaire de cardiologie et de pneumologie de Québec, Université Laval, Québec City, Québec, Canada
2. Department of Chemistry and Virginia Tech Center for Drug Discovery, Virginia Tech, Blacksburg, Virginia, USA
3. Faculty of Medicine, Université Laval, Québec City, Québec, Canada
4. University of Groningen, University Medical Center Groningen, Department of Pathology & Medical Biology, Experimental Pulmonology and Inflammation Research, Groningen, The Netherlands
5. University of Groningen, University Medical Center Groningen, GRIAC (Groningen Research Institute for Asthma and COPD), Groningen, The Netherlands
6. Department of Physiology and Pathophysiology, University of Manitoba, Winnipeg, MB, Canada
7. Biology of Breathing Group, Children's Hospital Research Institute of Manitoba, Winnipeg, MB, Canada

Corresponding author
David Marsolais
2725, chemin Ste-Foy, Québec, QC
Canada, G1V 4G5
Phone: 418-656-8711 x 3085
Fax: 418-656-4509
David.Marsolais@criucpq.ulaval.ca

Author Contribution
Participated in research design: PBL, SL, CAR, WLS, AJH, VJ, JS, DM
Conducted experiments: PBL, SL, CAR
Contributed new reagents: WS, JKB, AJH
Performed data analysis: PBL, SL, CAR, DM
Wrote or contributed to the writing: PBL, SL, CAR, WLS, AJH, VJ, JKB, JS, DM

Funding: This work was supported by CIHR grant # 274357 and funding from the Respiratory Health Network of Québec. PBL received a scholarship from the Sentinel North Strategy of the Canada First Research Excellence Fund. WLS is supported by the National Institutes of Health under grant R01GM121075. DM is a member of the FRQ-S Respiratory Health Network and receives a FRQ-S J2 research scholar award.

Running title: SphK2 substrate and airway smooth muscle cells

ABSTRACT

Thickening of the airway smooth muscle is central to bronchial hyperreactivity. We have shown that the sphingosine analog AAL-R can reverse pre-established airway hyperreactivity in a chronic asthma model. Since sphingosine analogs can be metabolized by sphingosine kinase 2, we investigated whether this enzyme was required for AAL-R to perturb mechanisms sustaining airway smooth muscle cell proliferation. We found that AAL-R pre-treatment reduced the capacity of live airway smooth muscle cells to use oxygen for oxidative phosphorylation and increased lactate dehydrogenase activity. We also determined that sphingosine kinase 2 was upregulated in airway smooth muscle cells bearing the proliferation marker Ki67, relative to their Ki67-negative counterpart. Comparing different stromal cell subsets of the lung, we found that high sphingosine kinase 2 levels were associated with the ability of AAL-R to inhibit metabolic activity assessed by conversion of the tetrazolium dye MTT. Knock down or pharmacologic inhibition of sphingosine kinase 2 reversed the effect of AAL-R on MTT conversion, indicating the essential role for this kinase in the metabolic perturbations induced by sphingosine analogs. Our results support the hypothesis that increased sphingosine kinase 2 levels in proliferating airway smooth muscle cells could be exploited to counteract airway smooth muscle thickening with synthetic substrates.

KEYWORDS

Asthma, sphingolipids, metabolism, AAL-R, FTY720

AJRCMB Articles in Press. Published on 27-June-2019 as 10.1165/rcmb.2018-0397OC

INTRODUCTION

Asthma is characterized by a thickening of the airway smooth muscle (ASM), which contributes prominently to airway narrowing (1). There is no existing pharmacological treatment specifically designed to impede ASM thickening in asthma, although corticosteroid can accelerate its resorption under specific conditions (2, 3). Both hyperplasia and hypertrophy of ASM cells are suspected to contribute to asthma pathogenesis (4). *In vitro*, ASM cells from asthmatics display a hyperproliferative and a hypersecretory phenotype (5, 6). Moreover, a number of studies have documented, at least in the distal airways, that cellular alterations compatible with heightened oxidative phosphorylation are associated with ASM enlargement, including increased mitochondrial numbers, mass, and oxygen consumption (7, 8).

Of critical importance is the notion that enhanced mitochondrial functions are required to sustain instrumental aspects of tissue hypertrophy such as protein synthesis (9) and proliferation (10). Interfering with mitochondrial functions was shown to alleviate vascular smooth muscle hyperproliferation in the context of pulmonary hypertension (11) and oxidative phosphorylation is increased during stromal cell proliferation (12). It is thus conceivable that dysregulating energy metabolism is ASM cells could produce salutary effects in the context of asthma.

Increasing evidence obtained in the context of oncology suggest that synthetic sphingosine analogs can act through SPHK2 -dependent and -independent pathways to hamper cellular accumulation (13, 14). We recently demonstrated that a sphingosine analog, as well as substrate for SPHK2, could reverse airway smooth muscle thickening

in experimental asthma; and that sub-toxic concentrations of this agent could induce ASM cell cytostasis *in vitro* (15). Nevertheless, the mechanisms underlying the propensity of SPHK2 substrates to impact ASM thickening remain unclear.

In this study, we determined that the SPHK2 substrate - AAL-R – causes metabolic alterations that precede the reduction of ASM cell accumulation *in vitro*. These include the alteration of overall oxidoreductase activity, the impairment of oxidative phosphorylation, and the enhancement of lactate dehydrogenase activity. Importantly, we found that SPHK2 expression was increased in ASM cells bearing the proliferation marker Ki67, and that SPHK2 knock down reversed the ability of AAL-R to alter their metabolic activity.

MATERIAL AND METHODS

Cell culture

Human primary ASM cells (CC-2576; Lonza, Walkersville, MD) were cultured in Dulbecco's Modified Eagle Medium (DMEM) containing 10% fetal bovine serum (unless otherwise indicated), non-essential amino acids and 1% penicillin/streptomycin, and plated at a density of $1.5x10^4$ cells / cm^2. Human primary epithelial cells obtained from a normal patient's biopsy (Chakir laboratory) were characterized and cultured as described (16) and plated at a density of $2.5x10^4$ cells / cm^2. Human primary arterial endothelial cells (302-05a, Cell applications, San Diego, CA) were cultured in endothelial cell growth medium (Lonza, CC-3202) and plated at a density of $2.5x10^4$ cells / cm^2. Primary hTERT-immortalized ASM cells from asthmatics were cultured as

AJRCMB Articles in Press. Published on 27-June-2019 as 10.1165/rcmb.2018-0397OC

described (5). Cells were used at passages 3 to 8. Crystal violet (17), BrdU, MTT, LDH activity and JC-10 assays, as well as p21 western blot, were performed according to manufacturer's instruction (described in supplementary material).

Reagents

AAL-R and SLM6031434 were graciously provided by Hugh Rosen and Webster Santos, respectively. VPC 23019 was purchased from Tocris Bioscience (Oakville, ON, Canada), and recombinant human FGF-2 and TGF-β1 were purchased from Peprotech (Montreal, QC, Canada).

siRNA transfection

ASM cells were seeded at a density of 1.5 x 10^4 cells per cm^2 and transfected using calcium-phosphate (18) for 24 h with 25 nM of mock siRNA (ThermoFisher) or SPHK2 siRNA (s32285, ThermoFisher). Cells were incubated with VEH or increasing concentrations of AAL-R for 24 h for the MTT assay; with VEH or 1 μM AAL-R for 5 h for lipid quantification using liquid chromatography tandem-mass spectrometry as described (15). SPHK2 levels were assessed by western blot (Polyclonal, Proteintech) (described in supplementary material).

Flow cytometry

SPHK2 immunoreactivity on ASM, epithelial and endothelial cells was assessed as described in supplementary material. ASM surface expression of GLUT1 (polyclonal, Novus Biologicals) was measured after a 24 h incubation with 1 μM AAL-R. Apoptosis

was assessed after 72 h incubation with AAL-R 1, 5 and 10 μM using Pacific Blue Annexin V (Biolegend, San Diego, CA).

Mitochondrial content and activity

Mitochondrial DNA quantification was assessed by quantitative polymerase chain reaction (qPCR) as described by Rooney et al. (19) and further detailed in supplementary material. Mitochondrial respiration was measured in intact ASM cells incubated in complete DMEM media with VEH or 1 μM AAL-R for 24 h, using the Oxygraph-2K (OROBOROS Instruments, Innsbruck, Austria) according to variations of published methods (20, 21). See supplementary material for the detailed protocol.

Statistical analyses

Data were expressed using averages ± SEM. After verifying homogeneity of variances and the assumption of normality, unpaired T tests or ANOVA were performed. Post hoc analyses were performed using the Sidak correction. When necessary, data were log transformed prior to performing parametric tests. Data of oxygen consumption for mitochondrial respiration was evaluated using a RM-ANOVA followed by Fischer multiple comparison tests. All tests were performed with the Prism v. 6.01 software (GraphPad Software, Inc.). The significance of p was set at 0.05 for all the tests.

AJRCMB Articles in Press. Published on 27-June-2019 as 10.1165/rcmb.2018-0397OC

RESULTS

Metabolic alterations induced by AAL-R precede cytostasis

Increasing evidence supports that alteration of energy metabolism by sphingosine analogs contribute to inhibit proliferation (13). We observed that AAL-R, at a concentration of 1 μM, diminished the tetrazolium dye MTT reduction to formazan by 38 % after 24 h of incubation compared to cells incubated with the vehicle (**Fig 1A**), suggesting a decreased cell number or an hampered metabolic activity. We determined that accumulation of ASM cells, measured using the crystal violet staining, was not decreased by AAL-R at that time point (**Fig 1B**), showing that the metabolic activity rather than the accumulation of cells was in play at this early time point. In agreement with our previous results (15), AAL-R significantly altered BrdU incorporation relative to vehicle at 48 h (**Fig 1C**), which occurred in absence of striking accumulation of Annexin V-positive cells over a 72 h incubation period (**Fig 1D**). Thus, it appears that a concentration of AAL-R sufficient to cause cytostasis, but not apoptosis, rapidly impacts on determinants of oxidoreductase activity in ASM cells.

AAL-R interferes with oxidative phosphorylation and promotes lactate dehydrogenase activity

Since MTT reduction depends on oxidoreductase activity, which can involve both mitochondrial-dependent and -independent events, we determined if AAL-R impacted on the ability of proliferating ASM cells to utilize oxygen (**Fig 2**). We first compared, as a surrogate for mitochondrial numbers per cell, the relative amount of the tRNA(Leu(UUR)) mitochondrial gene vs the β2-microglobulin nuclear gene between experimental conditions. We found that AAL-R did not reduce the tRNA(Leu(UUR)) / β2-

microglobulin ratio, which provides evidence that reduced numbers of mitochondria per cell did not account for the altered MTT conversion (**Fig 2A**). However, we determined that routine oxygen consumption was reduced by nearly 15% as a result of the altered capacity to use oxygen in order to generate ATP (OXPHOS; 27% decrease), rather than by increasing proton leak (not different from VEH) (**Fig 2B**). This was accompanied by a shift towards a glycolytic metabolism that was evidenced by an increased cell surface expression of GLUT1 (**Fig 2C**) and an increased LDH activity (**Fig 2D**). Consistent with increased markers of glycolysis, we determined that AAL-R increased mitochondrial membrane potential (**Fig 2E**) measured by incorporation of the JC-10 dye (22). We did not observe a modulation of p21 levels in response to AAL-R (**Fig 2F** and **Fig E1**), indicating that it did not operate by influencing nuclear targets of SPHK2 products. Together, these results support the hypothesis that AAL-R mitigates energy metabolism in ASM cells.

Proliferative ASM cells are susceptible to AAL-R-induced inhibition of MTT conversion

Most sphingosine analogs are preferentially phosphorylated by SPHK2, compared to SPHK1 (22). Since proliferation likely contributes to ASM thickening in asthma (4, 5, 23), we assessed the immunoreactivity for SPHK2 in ASM cells bearing the proliferation marker Ki67 (**Fig 3**). Ki67-positive ASM cells showed a more than twofold increase in SPHK2 immunoreactivity compared to their Ki67-negative counterparts (**Fig 3A-B)**, suggesting that proliferating ASM cells might feature an enhanced sensitivity to SPHK2 substrates. We thus tested the impact of AAL-R under two culture conditions known to promote ASM cell proliferation *in vitro*, namely 10% FBS (24, 25), and combined

AJRCMB Articles in Press. Published on 27-June-2019 as 10.1165/rcmb.2018-0397OC

FGF2/TGF-β (17); as well as in ASM cells cultured in complete medium containing 1% FBS into which they do not expand (**Fig 3C**). We found MTT conversion to be enhanced regardless of the anabolic stimulus compared to the cells cultured in 1% FBS. Moreover, AAL-R decreased the conversion of MTT by nearly 40% under both anabolic stimuli compared to vehicle. Of note, AAL-R marginally affected MTT conversion in cells incubated with 1% FBS, suggesting that proliferative cells featuring high SPHK2 levels are susceptible to AAL-R-induced metabolic alterations.

AAL-R preferentially affects cells with high SPHK2 levels

Phosphorylatable sphingosine analogs can be delivered in the airways of mice with limited histological impacts (26, 27). Yet, we recently showed that the dysregulated ASM compartment, as seen in the context of asthma, resorbs in the presence of phosphorylatable sphingosine analogs such as AAL-R (15), indicating that the ASM features elements of sensitivity to this type of agents. We thus compared the expression of SPHK2 in ASM cells and other prevalent stromal cell subsets of the lung, namely endothelial and epithelial cells. We found that immunoreactivity for SPHK2 is twice higher in ASM cells compared to epithelial or endothelial cells (**Fig 4A-B**). In line with the pattern of SPHK2 expression of ASM cells, epithelial and endothelial cell lines, we observed that AAL-R potently inhibited the conversion of MTT by 45% in ASM cells, while having limited effects in endothelial and epithelial cell lines (**Fig 4C**). These results suggest that stromal cells with high SPHK2 levels are susceptible to metabolic perturbations induced by SPHK2 substrates. We also confirmed that AAL-R reduced MTT conversion in ASM cells from asthma patients (**Fig 4D**).

AAL-R-induced alteration of MTT conversion depends on SPHK2

To determine whether the impact of AAL-R on MTT conversion is dependent on SPHK2, we employed complementary strategies. We first demonstrated that low concentrations of SLM6031434, a SPHK2 inhibitor known to interfere with the phosphorylation of sphingosine analogs *in vitro* (28), rescued proliferating ASM cells from AAL-R-induced inhibition of MTT conversion (**Fig 5A**). Similarly, the lack of effect of AAL-R was recapitulated by knocking down SPHK2 with siRNAs (**Fig 5B**). In line with the contention that changes in the kinetics of AFD-R accumulation (the phosphorylated form of AAL-R) shall critically affect the impact of AAL-R on ASM cell function, we determined that SPHK2 knock down reduced the AFD-R to AAL-R ratio by nearly 50% (**Fig 5C**). Of note, we also confirmed the efficacy of siRNAs to reduce the content of SPHK2 (**Fig 5D**).

ASM cells express $S1P_1$, $S1P_2$, and $S1P_3$ receptors (15). Because AFD-R can bind to all S1P receptors except $S1P_2$ (29), we investigated their involvement in the AAL-R-mediated effects (**Fig 5E**). As expected, AAL-R diminished MTT conversion in proliferating cells, compared to vehicle. Arguing against a prominent role for endogenous/medium-containing S1P acting on $S1P_1$ and $S1P_3$ for FBS-driven enhancement of MTT conversion, we found that the dual $S1P_1$ and $S1P_3$ antagonist VPC23019 (10μM) had no effect on MTT conversion in absence of AAL-R, when compared to vehicle. Moreover, VPC23019 failed to alleviate the AAL-R-induced alteration of MTT conversion, refuting S1P receptors involvement.

AJRCMB Articles in Press. Published on 27-June-2019 as 10.1165/rcmb.2018-0397OC

DISCUSSION

The ASM is at the core of asthma symptoms and its thickening results from the perpetual stimulation with numerous anabolic stimuli including growth factors, spasmogens, and immune modulators (30, 31). The persistent reduction of ASM thickening associated with the long-term benefits of bronchial thermoplasty indicates that punctual interventions directed against the ASM bear therapeutic potential (32-34). We showed that the SPHK2 substrate AAL-R potently reversed airway hyperresponsiveness in a corticosteroid-resistant model of asthma and induced human ASM cell cytostasis *in vitro* (15), suggesting that SPHK2 could be a therapeutically-amenable target for interfering with ASM enlargement.

The current study furthers this contention by unraveling the preferential efficacy of AAL-R to alter energy metabolism when ASM cells are under anabolic conditions. For that matter, we found that ASM cells undergoing proliferation upregulate SPHK2 and that pulmonary stromal cell subsets with the highest levels of SPHK2 are more sensitive to metabolic perturbations induced by AAL-R. Critically, we demonstrate that knocking down or inhibiting SPHK2 makes AAL-R impotent at interfering with the activity of ASM cells, showing that beneficial effects depend on SPHK2.

If SPHK2 is increased in ASM cells under anabolic conditions, then why hasn't it come out in the omic studies of asthma? In our view, the most important factor masking the relationship between SPHK2 and asthma is that mild, but not severe SPHK2 overexpression sustains hyperproliferation (35). These findings are consistent with our own observation that ASM cells upregulate SPHK2 by merely twofold, when

proliferating. SPHK2 could thus be required for altering anabolic responses without affecting quiescent cells. In line with the usual caveats of omic studies performed on whole tissue samples, SPHK2 is not equally expressed in the different cell types of the lung, which is confirmed by our *in vitro* findings exposing unequal SPHK2 immunoreactivity between ASM cells, endothelial and epithelial cells. Although our study was performed with a limited number of cell lines, our results clearly demonstrate that AAL-R can alter MTT signal in ASM cells from asthma patients; and that cell lines with the highest levels of SPHK2 are the most susceptible to the metabolic perturbations induced by a SPHK2 substrate. Together with our previous *in vivo* findings showing that AAL-R does not cause aversive effects in the airways while reversing hyperresponsiveness (15), the results of the current study argue that mild overexpression of SPHK2 in ASM cells under anabolic conditions increases their susceptibility to AAL-R-induced metabolic perturbations.

This notion is also corroborated by the fact that SPHK2 substrates with the intrinsic propensity to rapidly accumulate into cells are the most potent at inhibiting MTT conversion and/or cell accumulation (13, 36, 37). In the same line of thoughts, the sensitivity to rapidly-phosphorylated SPHK2 substrates correlates with the level of SPHK2 expression in cancer cells (13). The correlation between SPHK2 expression and sensitivity to SPHK2 substrates also aligns with our observation that a partial knock down of SPHK2, which leads to a 50% decrease of the AFD-R to AAL-R ratio, abrogated the impact of low micromolar concentrations of AAL-R on MTT conversion. In addition, concentrations of the SPHK2 inhibitor SLM6031434 lower than its documented IC50 were sufficient to halt AAL-R-induced perturbation of MTT conversion (28).

AJRCMB Articles in Press. Published on 27-June-2019 as 10.1165/rcmb.2018-0397OC

Therefore, our study strengthens the notion that asthma-related increase of SPHK2, or alternatively that means of promoting SPHK2 expression in the airway smooth muscle, could serve as a basis to counteract asthma with SPHK2 substrates.

The current study also supports the contention that the ability of sphingosine analogs to interfere with ASM thickening likely not involve the activation/reactivation of protein phosphatases. Indeed, it was shown that AAL-S, an isomer of AAL-R that is not a SPHK2 substrate, inhibited the development of experimental asthma by a mechanism involving the promotion of protein phosphatase activity, leading to the inhibition of inflammatory mediators release (38). Importantly, intracellular accumulation of the non-phosphorylated form of sphingosine analogs was also shown to promote protein phosphatase activity in cancer cell lines, which led to their decreased accumulation through the inhibition of nutrient intake (37). For that matter, it is increasingly clear that sphingosine analogs poorly metabolized by SPHK2 preferentially promote protein phosphatase activity, when compared to rapidly-metabolized substrates, like AAL-R (37). Our finding that AAL-R loses its ability to interfere with ASM cell metabolism when SPHK2 is knocked down, combined to no inhibition of cell surface expression of GLUT1, argue that the mechanisms of action likely not rely on the promotion of protein phosphatase activity.

Although cells deficient for SPHK2 were documented to display an altered mitochondrial function (39), we were not surprised that SPHK2 knock down or pharmacological inhibition did not impact on basal MTT conversion. In fact, it appears that mitochondrial impacts of SPHK2 knock down are highly dependent on the system, with fully knocked

out cardiomyocytes displaying a mere 20% inhibition of complex IV-associated O_2 consumption, and partial SPHK2 knock down in Hela cells yielding a more than 50% inhibitory effect (39). Our results suggest that the metabolic effects of SPHK2 substrates exceed the impact of SPHK2 modulators in perturbing mitochondrial functions under the current experimental conditions.

Our study indicates that the mechanisms of action of synthetic SPHK2 substrates overlap with some of the functions of the endogenous substrate (sphingosine). Indeed, we determined that the decreased oxygen consumption caused by AAL-R led to mitochondrial membrane hyperpolarity. Since endogenous S1P inhibits the depolarisation of the mitochondrial membrane in response to hypoxic episodes (40), it is possible that the phosphorylated form of AAL-R acts as an intracellular S1P mimic in order to prevent the loss of mitochondrial membrane potential and thus prevent cell death. Although this theory will require further investigation, we determined that AAL-R induced an upregulation of GLUT1 at the cell surface, an event that also confers protection against apoptosis in situations where oxidative metabolism is altered (41, 42). Altogether, our results support the hypothesis that SPHK2 substrates are modulators of energy metabolism, and evidence that they trigger compensatory mechanisms usually associated with hypoxia that likely prevent mitochondrion-associated cell death.

CONCLUSION

Although reversing the thickening of the ASM is likely to improve asthma in a majority of patients, there is currently no clinically-approved pharmacological strategies that directly target the ASM. The task of identifying such strategy is made complex by the subtle

AJRCMB Articles in Press. Published on 27-June-2019 as 10.1165/rcmb.2018-0397OC

phenotypical changes seen in ASM cells from patients *in vitro*, by the fact that mechanisms promoting and sustaining ASM thickening are numerous, interacting, and thus not finite. Our findings have unravelled that SPHK2 levels are increased in ASM cells subjected to anabolic stimuli. In line with the central role of sphingolipids in regulating cell fate and metabolism, our study supports the concept that this upregulation could be employed to interfere with the anabolically-skewed profile of the ASM in asthma.

ACKNOWLEDGEMENTS

We thank Sophie Plante and Jamila Chakir for providing the epithelial cells.

AJRCMB Articles in Press. Published on 27-June-2019 as 10.1165/rcmb.2018-0397OC

REFERENCES

1. Lauzon AM, Martin JG. Airway hyperresponsiveness; smooth muscle as the principal actor. *F1000Res* 2016; 5.

2. Berair R, Brightling CE. Asthma therapy and its effect on airway remodelling. *Drugs* 2014; 74: 1345-1369.

3. Leclere M, Lavoie-Lamoureux A, Joubert P, Relave F, Setlakwe EL, Beauchamp G, Couture C, Martin JG, Lavoie JP. Corticosteroids and antigen avoidance decrease airway smooth muscle mass in an equine asthma model. *Am J Respir Cell Mol Biol* 2012; 47: 589-596.

4. James AL, Elliot JG, Jones RL, Carroll ML, Mauad T, Bai TR, Abramson MJ, McKay KO, Green FH. Airway smooth muscle hypertrophy and hyperplasia in asthma. *Am J Respir Crit Care Med* 2012; 185: 1058-1064.

5. Burgess JK, Ketheson A, Faiz A, Limbert Rempel KA, Oliver BG, Ward JPT, Halayko AJ. Phenotype and Functional Features of Human Telomerase Reverse Transcriptase Immortalized Human Airway Smooth Muscle Cells from Asthmatic and Non-Asthmatic Donors. *Sci Rep* 2018; 8: 805.

6. Hassan M, Jo T, Risse PA, Tolloczko B, Lemiere C, Olivenstein R, Hamid Q, Martin JG. Airway smooth muscle remodeling is a dynamic process in severe long-standing asthma. *J Allergy Clin Immunol* 2010; 125: 1037-1045 e1033.

7. Girodet PO, Allard B, Thumerel M, Begueret H, Dupin I, Ousova O, Lassalle R, Maurat E, Ozier A, Trian T, Marthan R, Berger P. Bronchial Smooth Muscle Remodeling in Nonsevere Asthma. *Am J Respir Crit Care Med* 2016; 193: 627-633.

8. Trian T, Benard G, Begueret H, Rossignol R, Girodet PO, Ghosh D, Ousova O, Vernejoux JM, Marthan R, Tunon-de-Lara JM, Berger P. Bronchial smooth muscle remodeling involves calcium-dependent enhanced mitochondrial biogenesis in asthma. *J Exp Med* 2007; 204: 3173-3181.

9. Vishnu N, Jadoon Khan M, Karsten F, Groschner LN, Waldeck-Weiermair M, Rost R, Hallstrom S, Imamura H, Graier WF, Malli R. ATP increases within the lumen of the endoplasmic reticulum upon intracellular Ca2+ release. *Mol Biol Cell* 2014; 25: 368-379.

10. Yu M, Shi Y, Wei X, Yang Y, Zhou Y, Hao X, Zhang N, Niu R. Depletion of mitochondrial DNA by ethidium bromide treatment inhibits the proliferation and tumorigenesis of T47D human breast cancer cells. *Toxicol Lett* 2007; 170: 83-93.

11. Boucherat O, Peterlini T, Bourgeois A, Nadeau V, Breuils-Bonnet S, Boilet-Molez S, Potus F, Meloche J, Chabot S, Lambert C, Tremblay E, Chae YC, Altieri DC, Sutendra G, Michelakis ED, Paulin R, Provencher S, Bonnet S. Mitochondrial HSP90 Accumulation Promotes Vascular Remodeling in Pulmonary Arterial Hypertension. *Am J Respir Crit Care Med* 2018.

AJRCMB Articles in Press. Published on 27-June-2019 as 10.1165/rcmb.2018-0397OC

12. Yao CH, Wang R, Wang Y, Kung CP, Weber JD, Patti GJ. Mitochondrial fusion supports increased oxidative phosphorylation during cell proliferation. *Elife* 2019; 8.

13. McCracken AN, McMonigle RJ, Tessier J, Fransson R, Perryman MS, Chen B, Keebaugh A, Selwan E, Barr SA, Kim SM, Roy SG, Liu G, Fallegger D, Sernissi L, Brandt C, Moitessier N, Snider AJ, Clare S, Muschen M, Huwiler A, Kleinman MT, Hanessian S, Edinger AL. Phosphorylation of a constrained azacyclic FTY720 analog enhances anti-leukemic activity without inducing S1P receptor activation. *Leukemia* 2017; 31: 669-677.

14. Romero Rosales K, Singh G, Wu K, Chen J, Janes MR, Lilly MB, Peralta ER, Siskind LJ, Bennett MJ, Fruman DA, Edinger AL. Sphingolipid-based drugs selectively kill cancer cells by down-regulating nutrient transporter proteins. *Biochem J* 2011; 439: 299-311.

15. Gendron DR, Lecours PB, Lemay AM, Beaulieu MJ, Huppe CA, Lee-Gosselin A, Flamand N, Don AS, Bissonnette E, Blanchet MR, Laplante M, Bourgoin SG, Bosse Y, Marsolais D. A Phosphorylatable Sphingosine Analog Induces Airway Smooth Muscle Cytostasis and Reverses Airway Hyperresponsiveness in Experimental Asthma. *Front Pharmacol* 2017; 8: 78.

16. Goulet F, Boulet LP, Chakir J, Tremblay N, Dube J, Laviolette M, Boutet M, Xu W, Germain L, Auger FA. Morphologic and functional properties of bronchial cells

isolated from normal and asthmatic subjects. *Am J Respir Cell Mol Biol* 1996; 15: 312-318.

17. Bosse Y, Thompson C, Stankova J, Rola-Pleszczynski M. Fibroblast growth factor 2 and transforming growth factor beta1 synergism in human bronchial smooth muscle cell proliferation. *Am J Respir Cell Mol Biol* 2006; 34: 746-753.

18. Margolskee RF, McHendry-Rinde B, Horn R. Panning transfected cells for electrophysiological studies. *Biotechniques* 1993; 15: 906-911.

19. Rooney JP, Ryde IT, Sanders LH, Howlett EH, Colton MD, Germ KE, Mayer GD, Greenamyre JT, Meyer JN. PCR based determination of mitochondrial DNA copy number in multiple species. *Methods Mol Biol* 2015; 1241: 23-38.

20. Gnaiger E. Mitochondrial Pathways and Respiratory Control: An Introduction to OXPHOS Analysis. In: Corp OI, editor, 4th edition ed. Innsbruck, Austria: OROBOROS MiPNet Publications; 2014.

21. Laouafa S, Roussel D, Marcouiller F, Soliz J, Bairam A, Joseph V. Role of Estradiol Receptor Beta (ER beta) on Brain Mitochondrial Functions and Cardio-respiratory Control in Aged Female Mice. In: journal TF, editor. Experimental Biology 2018 Meeting. San Diego; 2018.

AJRCMB Articles in Press. Published on 27-June-2019 as 10.1165/rcmb.2018-0397OC

22. Billich A, Bornancin F, Devay P, Mechtcheriakova D, Urtz N, Baumruker T. Phosphorylation of the immunomodulatory drug FTY720 by sphingosine kinases. *J Biol Chem* 2003; 278: 47408-47415.

23. Johnson PR, Roth M, Tamm M, Hughes M, Ge Q, King G, Burgess JK, Black JL. Airway smooth muscle cell proliferation is increased in asthma. *Am J Respir Crit Care Med* 2001; 164: 474-477.

24. Chen G, Khalil N. TGF-beta1 increases proliferation of airway smooth muscle cells by phosphorylation of map kinases. *Respir Res* 2006; 7: 2.

25. Mahn K, Hirst SJ, Ying S, Holt MR, Lavender P, Ojo OO, Siew L, Simcock DE, McVicker CG, Kanabar V, Snetkov VA, O'Connor BJ, Karner C, Cousins DJ, Macedo P, Chung KF, Corrigan CJ, Ward JP, Lee TH. Diminished sarco/endoplasmic reticulum Ca2+ ATPase (SERCA) expression contributes to airway remodelling in bronchial asthma. *Proc Natl Acad Sci U S A* 2009; 106: 10775-10780.

26. Gendron D, Lemay AM, Tremblay C, Lai LJ, Langlois A, Bernatchez E, Flamand N, Blanchet MR, Don AS, Bosse Y, Bissonnette E, Marsolais D. Treatment with a sphingosine analog after the inception of house dust mite-induced airway inflammation alleviates key features of experimental asthma. *Respir Res* 2015; 16: 7.

27. Idzko M, Hammad H, van Nimwegen M, Kool M, Muller T, Soullie T, Willart MA, Hijdra D, Hoogsteden HC, Lambrecht BN. Local application of FTY720 to the lung

abrogates experimental asthma by altering dendritic cell function. *J Clin Invest* 2006; 116: 2935-2944.

28. Kharel Y, Morris EA, Congdon MD, Thorpe SB, Tomsig JL, Santos WL, Lynch KR. Sphingosine Kinase 2 Inhibition and Blood Sphingosine 1-Phosphate Levels. *J Pharmacol Exp Ther* 2015; 355: 23-31.

29. Brinkmann V, Davis MD, Heise CE, Albert R, Cottens S, Hof R, Bruns C, Prieschl E, Baumruker T, Hiestand P, Foster CA, Zollinger M, Lynch KR. The immune modulator FTY720 targets sphingosine 1-phosphate receptors. *J Biol Chem* 2002; 277: 21453-21457.

30. Elliot JG, Noble PB, Mauad T, Bai TR, Abramson MJ, McKay KO, Green FHY, James AL. Inflammation-dependent and independent airway remodelling in asthma. *Respirology* 2018.

31. Bosse Y. Asthmatic airway hyperresponsiveness: the ants in the tree. *Trends Mol Med* 2012; 18: 627-633.

32. Donovan GM, Elliot JG, Green FHY, James AL, Noble PB. Unraveling a Clinical Paradox: Why Does Bronchial Thermoplasty Work in Asthma? *Am J Respir Cell Mol Biol* 2018; 59: 355-362.

AJRCMB Articles in Press. Published on 27-June-2019 as 10.1165/rcmb.2018-0397OC

33. Pretolani M, Dombret MC, Thabut G, Knap D, Hamidi F, Debray MP, Taille C, Chanez P, Aubier M. Reduction of airway smooth muscle mass by bronchial thermoplasty in patients with severe asthma. *Am J Respir Crit Care Med* 2014; 190: 1452-1454.

34. Wechsler ME, Laviolette M, Rubin AS, Fiterman J, Lapa e Silva JR, Shah PL, Fiss E, Olivenstein R, Thomson NC, Niven RM, Pavord ID, Simoff M, Hales JB, McEvoy C, Slebos DJ, Holmes M, Phillips MJ, Erzurum SC, Hanania NA, Sumino K, Kraft M, Cox G, Sterman DH, Hogarth K, Kline JN, Mansur AH, Louie BE, Leeds WM, Barbers RG, Austin JH, Shargill NS, Quiring J, Armstrong B, Castro M, Asthma Intervention Research 2 Trial Study G. Bronchial thermoplasty: Long-term safety and effectiveness in patients with severe persistent asthma. *J Allergy Clin Immunol* 2013; 132: 1295-1302.

35. Neubauer HA, Pham DH, Zebol JR, Moretti PA, Peterson AL, Leclercq TM, Chan H, Powell JA, Pitman MR, Samuel MS, Bonder CS, Creek DJ, Gliddon BL, Pitson SM. An oncogenic role for sphingosine kinase 2. *Oncotarget* 2016; 7: 64886-64899.

36. Don AS, Martinez-Lamenca C, Webb WR, Proia RL, Roberts E, Rosen H. Essential requirement for sphingosine kinase 2 in a sphingolipid apoptosis pathway activated by FTY720 analogues. *The Journal of biological chemistry* 2007; 282: 15833-15842.

37. Kim SM, Roy SG, Chen B, Nguyen TM, McMonigle RJ, McCracken AN, Zhang Y, Kofuji S, Hou J, Selwan E, Finicle BT, Nguyen TT, Ravi A, Ramirez MU, Wiher T,

Guenther GG, Kono M, Sasaki AT, Weisman LS, Potma EO, Tromberg BJ, Edwards RA, Hanessian S, Edinger AL. Targeting cancer metabolism by simultaneously disrupting parallel nutrient access pathways. *J Clin Invest* 2016; 126: 4088-4102.

38. Collison A, Hatchwell L, Verrills N, Wark PA, de Siqueira AP, Tooze M, Carpenter H, Don AS, Morris JC, Zimmermann N, Bartlett NW, Rothenberg ME, Johnston SL, Foster PS, Mattes J. The E3 ubiquitin ligase midline 1 promotes allergen and rhinovirus-induced asthma by inhibiting protein phosphatase 2A activity. *Nat Med* 2013; 19: 232-237.

39. Strub GM, Paillard M, Liang J, Gomez L, Allegood JC, Hait NC, Maceyka M, Price MM, Chen Q, Simpson DC, Kordula T, Milstien S, Lesnefsky EJ, Spiegel S. Sphingosine-1-phosphate produced by sphingosine kinase 2 in mitochondria interacts with prohibitin 2 to regulate complex IV assembly and respiration. *FASEB J* 2011; 25: 600-612.

40. Gomez L, Paillard M, Price M, Chen Q, Teixeira G, Spiegel S, Lesnefsky EJ. A novel role for mitochondrial sphingosine-1-phosphate produced by sphingosine kinase-2 in PTP-mediated cell survival during cardioprotection. *Basic Res Cardiol* 2011; 106: 1341-1353.

41. Malhotra R, Tyson DG, Sone H, Aoki K, Kumagai AK, Brosius FC, 3rd. Glucose uptake and adenoviral mediated GLUT1 infection decrease hypoxia-induced HIF-1alpha levels in cardiac myocytes. *J Mol Cell Cardiol* 2002; 34: 1063-1073.

AJRCMB Articles in Press. Published on 27-June-2019 as 10.1165/rcmb.2018-0397OC

42. Zhu H, Xue H, Jin QH, Guo J, Chen YD. MiR-138 protects cardiac cells against hypoxia through modulation of glucose metabolism by targetting pyruvate dehydrogenase kinase 1. *Biosci Rep* 2017; 37.

FIGURE LEGENDS

Figure 1. A cytostatic concentration of AAL-R inhibits metabolic activity of ASM cells. Primary human ASM cells were incubated with vehicle (VEH) or AAL-R in complete media containing 10% FBS. **A)** A 24 h incubation with AAL-R (1 μM) decreased MTT conversion, which occurred **B**) without modulation of ASM cell accumulation. **C**) After 48 h of incubation, AAL-R (1 μM) reduced BrdU incorporation compared to the vehicle. **D**) These alterations occurred without significant induction of apoptosis over 72 h. n= 3-8, *: $p<0.05$ compared to VEH.

Figure 2. AAL-R causes a shift towards glycolytic metabolism. A-B) Primary human ASM cells were incubated for 24 h with vehicle (VEH) or AAL-R (1 μM) in complete medium containing 10% FBS. AAL-R did not modify **A)** the ratio between genomic mitochondrial and nuclear housekeeping gene levels. **B)** Microoxymetry was performed in VEH and AAL-R-treated cells in order to derive O_2 consumption associated with routine respiration, proton leak (state 4), OXPHOS (state 3) and maximal respiration, as described in methods. **C**) AAL-R (1 μM) led to the increase of GLUT1 and **D**) increased LHD activity after 24h. **E**) AAL-R increased JC-10 aggregates (red/green ratio) at 24h (FCCP 20 μM was used as a positive control) but **F**) had no impact on p21 expression at 6 and 18h. n= 3-8, *: $p<0.05$ compared to VEH.

Figure 3. SPHK2 overexpression in proliferative ASM cells sensitizes to inhibition of MTT conversion by AAL-R. A-B) Median fluorescence intensity (MFI) for SPHK2 is

AJRCMB Articles in Press. Published on 27-June-2019 as 10.1165/rcmb.2018-0397OC

higher in Ki-positive ($Ki67^+$) proliferative primary human ASM cells compared to Ki-negative (Ki^-) cells. **C)** The impact of a 24 h exposure to vehicle (VEH) or AAL-R (1 μM) on MTT conversion was assessed in primary human ASM cells incubated in complete medium containing 10% FBS in FBS-free medium containing FGF-2 and TGF-β1 or in medium containing 1% FBS. n= 3-8, *: $p<0.05$ compared to VEH.

Figure 4. The inhibition of MTT conversion by AAL-R preferentially impacts on stromal cells with high SPHK2 expression. Primary human ASM, endothelial, epithelial and hTERT-immortalized ASM cells isolated from asthma patients were incubated in complete media containing 10% FBS. **A-B**) Flow cytometric analyses of SPHK2 immunoreactivity in proliferative primary human ASM cells compared to primary human endothelial cells and epithelial cells. **C**) ASM cells, but not endothelial and epithelial cells, show a decreased MTT conversion in response to AAL-R (1 μM) after 24 h, compared to VEH. **D**) AAL-R (1 μM; 24 h) induces a decreased MTT conversion in hTERT-immortalized ASM cells from three different asthma patients (P1 to P3). n= 3-8, *: $p<0.05$.

Figure 5. The inhibition of MTT conversion by AAL-R depends on SPHK2 but does not involve S1P receptors 1 to 3. Primary human ASM cells were incubated for 24 h with vehicle (VEH) or AAL-R (1 μM) in complete medium containing 10% FBS and **A**) the sphingosine kinase inhibitor SLM6031434. **B**) SPHK2 knockdown by siRNAs interferes with the loss of MTT signal induced by AAL-R when compared to mock-transfected cells. **C**) Compared to mock-transfected cells, SPHK2 siRNA transfection reduced the phosphorylation of AAL-R to AFD-R. **D**) The efficiency of siRNAs against

SPHK2 was confirmed by western blots. **E**) The impact of a 24 h incubation with AAL-R (1 μM) on MTT conversion is not modified by the dual $S1P_{1-3}$ antagonist VPC23019 (10 μM). n= 3-8, *: $p<0.05$ compared to VEH.

AJRCMB Articles in Press. Published on 27-June-2019 as 10.1165/rcmb.2018-0397OC

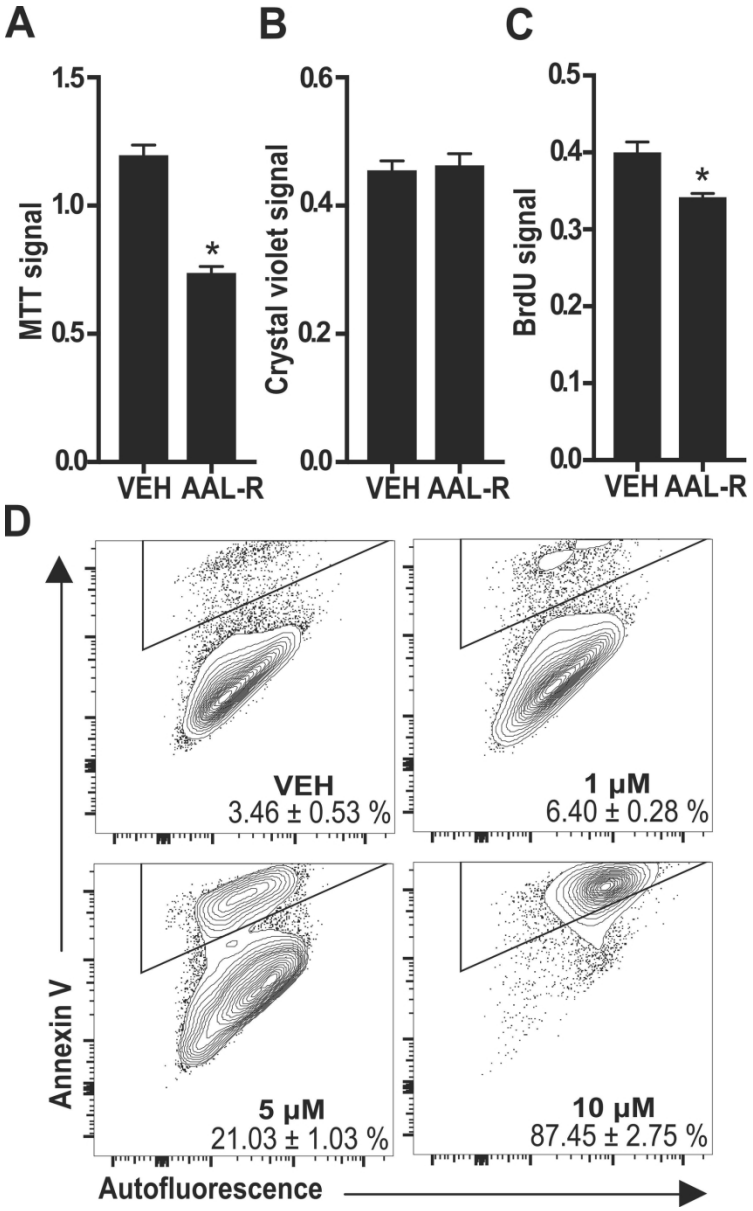

Figure 1. A cytostatic concentration of AAL-R inhibits metabolic activity of ASM cells. Primary human ASM cells were incubated with vehicle (VEH) or AAL-R in complete media containing 10% FBS. A) A 24 h incubation with AAL-R (1 µM) decreased MTT conversion, which occurred B) without modulation of ASM cell accumulation. C) After 48 h of incubation, AAL-R (1 µM) reduced BrdU incorporation compared to the vehicle. D) These alterations occurred without significant induction of apoptosis over 72 h. n= 3-8, *: $p<0.05$ compared to VEH.

73x118mm (600 x 600 DPI)

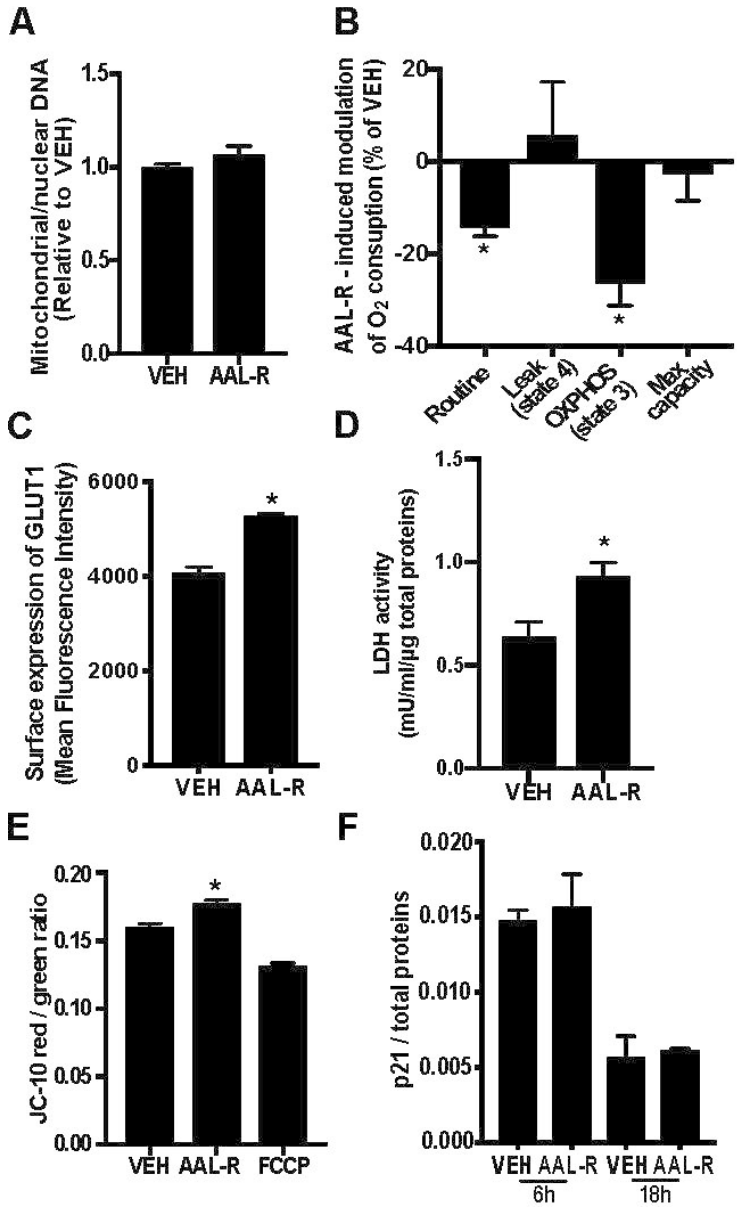

Figure 2. AAL-R causes a shift towards glycolytic metabolism. A-B) Primary human ASM cells were incubated for 24 h with vehicle (VEH) or AAL-R (1 µM) in complete medium containing 10% FBS. AAL-R did not modify A) the ratio between genomic mitochondrial and nuclear housekeeping gene levels. B) Microoxymetry was performed in VEH and AAL-R-treated cells in order to derive O2 consumption associated with routine respiration, proton leak (state 4), OXPHOS (state 3) and maximal respiration, as described in methods. C) AAL-R (1 µM) led to the increase of GLUT1 and D) increased LHD activity after 24h. E) AAL-R increased JC-10 aggregates (red/green ratio) at 24h (FCCP 20 µM was used as a positive control) but F) had no impact on p21 expression at 6 and 18h. n= 3-8, *: $p<0.05$ compared to VEH.

82x133mm (200 x 200 DPI)

AJRCMB Articles in Press. Published on 27-June-2019 as 10.1165/rcmb.2018-0397OC

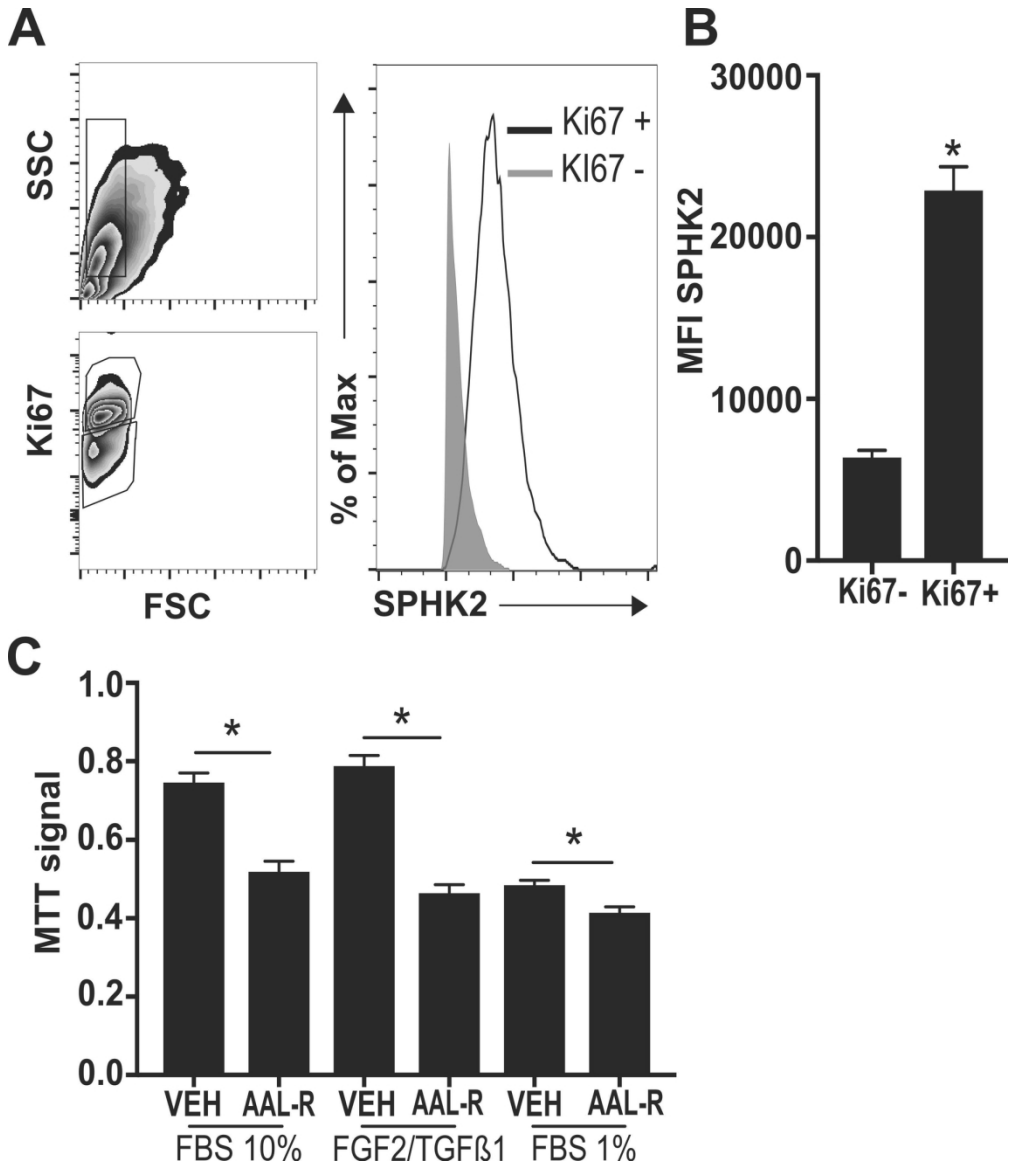

Figure 3. SPHK2 overexpression in proliferative ASM cells sensitizes to inhibition of MTT conversion by AAL-R. A-B) Median fluorescence intensity (MFI) for SPHK2 is higher in Ki-positive (Ki67+) proliferative primary human ASM cells compared to Ki-negative (Ki-) cells. C) The impact of a 24 h exposure to vehicle (VEH) or AAL-R (1 μM) on MTT conversion was assessed in primary human ASM cells incubated in complete medium containing 10% FBS in FBS-free medium containing FGF-2 and TGF-β1 or in medium containing 1% FBS. n= 3-8, *: $p<0.05$ compared to VEH.

80x93mm (600 x 600 DPI)

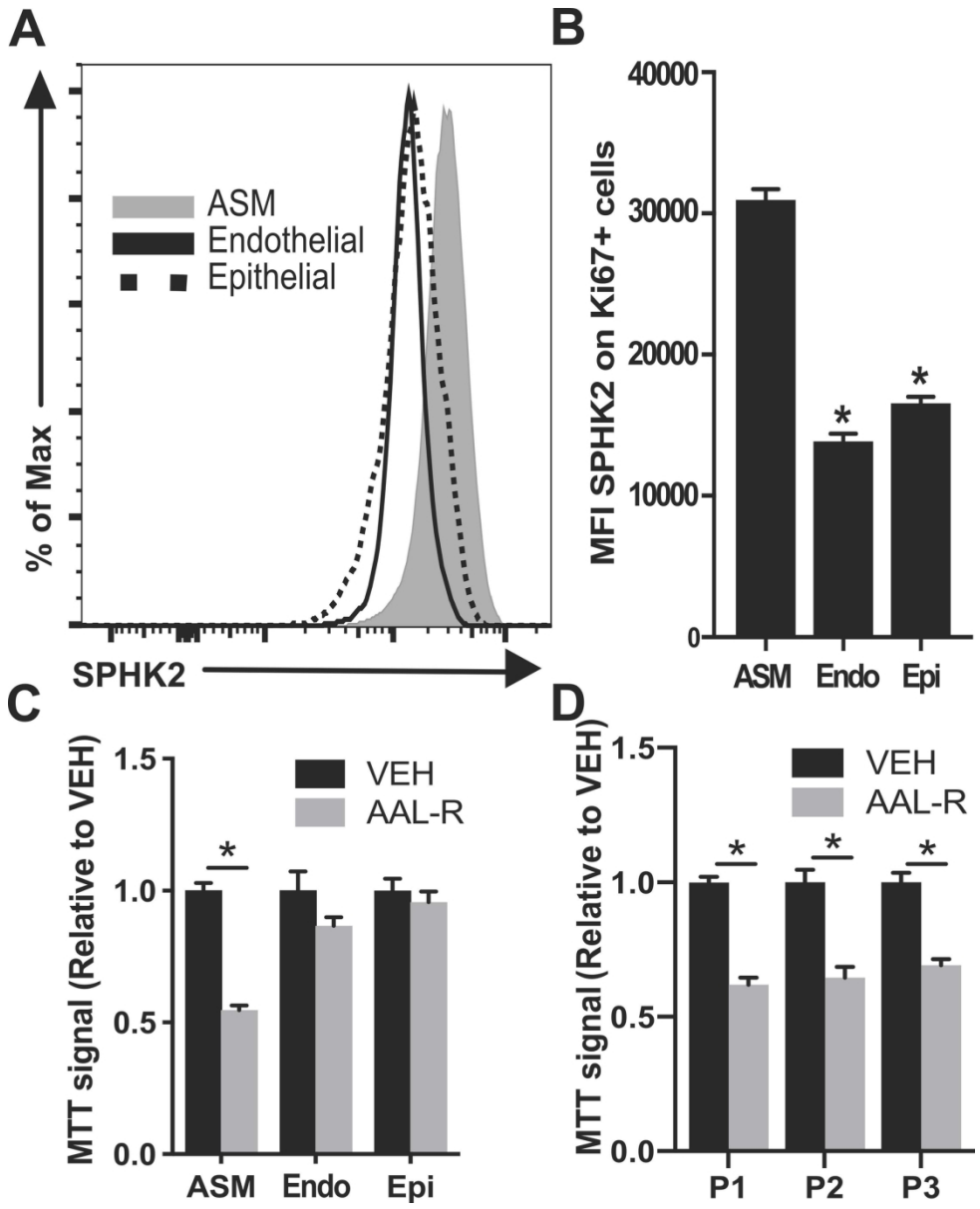

Figure 4. The inhibition of MTT conversion by AAL-R preferentially impacts on stromal cells with high SPHK2 expression. Primary human ASM, endothelial, epithelial and hTERT-immortalized ASM cells isolated from asthma patients were incubated in complete media containing 10% FBS. A-B) Flow cytometric analyses of SPHK2 immunoreactivity in proliferative primary human ASM cells compared to primary human endothelial cells and epithelial cells. C) ASM cells, but not endothelial and epithelial cells, show a decreased MTT conversion in response to AAL-R (1 μM) after 24 h, compared to VEH. D) AAL-R (1 μM; 24 h) induces a decreased MTT conversion in hTERT-immortalized ASM cells from three different asthma patients (P1 to P3). n= 3-8, *: $p<0.05$.

79x98mm (600 x 600 DPI)

AJRCMB Articles in Press. Published on 27-June-2019 as 10.1165/rcmb.2018-0397OC

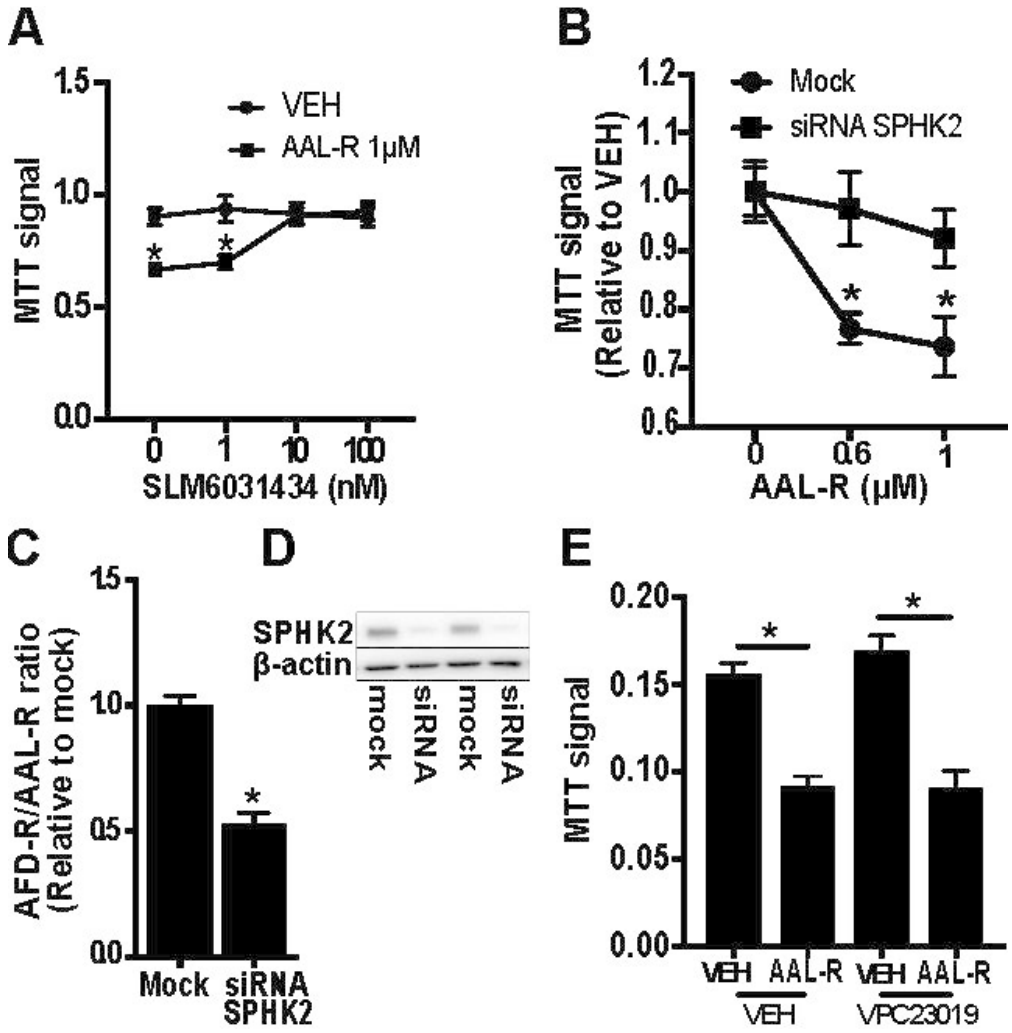

Figure 5. The inhibition of MTT conversion by AAL-R depends on SPHK2 but does not involve S1P receptors 1 to 3. Primary human ASM cells were incubated for 24 h with vehicle (VEH) or AAL-R (1 µM) in complete medium containing 10% FBS and A) the sphingosine kinase inhibitor SLM6031434. B) SPHK2 knockdown by siRNAs interferes with the loss of MTT signal induced by AAL-R when compared to mock-transfected cells. C) Compared to mock-transfected cells, SPHK2 siRNA transfection reduced the phosphorylation of AAL-R to AFD-R. D) The efficiency of siRNAs against SPHK2 was confirmed by western blots. E) The impact of a 24 h incubation with AAL-R (1 µM) on MTT conversion is not modified by the dual S1P1-3 antagonist VPC23019 (10 µM). n= 3-8, *: $p<0.05$ compared to VEH.

81x83mm (200 x 200 DPI)

AJRCMB Articles in Press. Published on 27-June-2019 as 10.1165/rcmb.2018-0397OC

Metabolic adaptation of airway smooth muscle cells to a SPHK2 substrate precedes cytostasis

Pascale Blais-Lecours[1], Sofien Laouafa[1], Christian Arias-Reyes[1], Webster L. Santos[2], Vincent Joseph[1,3], Janette K. Burgess[4,5], Andrew J. Halayko[6,7], Jorge Soliz[1,3] and David Marsolais[1,3]

ONLINE DATA SUPPLEMENT

Material and Methods

BrdU, MTT, crystal violet, JC-10 and LDH activity assays

The Sigma-Aldrich colorimetric BrdU cell proliferation assay was used to quantify DNA synthesis as described by the manufacturer (Millipore Sigma, Oakville, ON, Canada). To quantify metabolic activity, cells were incubated in fresh media with 1 mM of tetrazolium dye MTT (3-(4,5-dimethylthiazol-2-yl)-2,5-diphenyltetrazolium bromide) (Millipore Sigma) for 4 h at 37°C and formazan formation was measured by spectrophotometry at 540 nm after cell disruption with DMSO. Cell accumulation after AAL-R exposure was quantified by the crystal violet assay as described (1). Mitochondria membrane potential was measured using the JC-10 dye (Millipore Sigma, St-Louis, MO) following manufacturer's instructions. Briefly, ASM cells were incubated in complete DMEM media with VEH or with 1 µM AAL-R for 24 h, or with 20 µM of the uncoupling agent FCCP for 10 min, prior to the incubation for 60 min with JC-10. The ratio of red fluorescence (polarized mitochondrial membrane) over green fluorescence (low membrane potential) was then measured by spectrophotometry. Lactate dehydrogenase (LDH) activity of ASM cells incubated in complete DMEM media with VEH or with 1 µM AAL-R for 24 h was measured using the colorimetric LDH Assay kit (Abcam, Cambridge, UK).

AJRCMB Articles in Press. Published on 27-June-2019 as 10.1165/rcmb.2018-0397OC

Western blots

Cells were washed with PBS and lysed in buffer containing 1M HEPES, 4M NaCl, 100 mM GDTA, 200 mM NaVO4, 1M NaF, 83.3 mM Na pyrophosphate, 500 mM Na beta glycerophosphate, protease inhibitor (complete Mini EDTA-free Protease Inhibitor Cocktail, Millipore Sigma), 10 mg/ml sodium deoxycholate, 1% NP40 and 10% SDS. 10 to 15 µg of protein were loaded in 10% acrylamide gel for protein separation, transferred on a PVDF or nitrocellulose membrane and labeled overnight at 4°C with the rabbit anti-SPHK2 antibody (Polyclonal, Proteintech), rabbit anti-p21 antibody (Monoclonal, Cell Signaling Technology) and the control protein antibody mouse anti-β-actin (Clone AC-15, Sigma-Aldrich). Membranes were then incubated with horseradish peroxidase-coupled anti-rabbit (Cell Signaling Technology) or anti-mouse (BD Biosciences) IgG, or with the IRDye 800 CW goat anti-rabbit IgG (LI-COR Biosciences), and signal was revealed with ECL Luminata Crescendo (EMD Millipore) and the ChemiDoc apparatus (Bio-Rad Laboratories, Mississauga, ON, Canada), or with the REVERT total protein stain (LI-COR Biosciences) and the Odyssey LI-COR apparatus (LI-COR Biosciences, Lincoln, Nebraska).

Flow cytometry

To quantify SPHK2 immunoreactivity, cells were grown to obtain a pool of 75% (proliferative) and 100% (non-proliferative) cell confluence, permeabilized with the Foxp3 transcription factor staining buffer kit (eBioscience) and stained with primary antibodies raised against Ki67 (SolA15, eBioscience) and SPHK2 (Polyclonal, Proteintech, Rosemont, IL). Data were acquired using a FACS Diva-driven LSR Fortessa (BD,

Franklin Lake, NJ, USA) and analyzed with the FlowJo software (Tree Star Inc, Ashland, OR, USA).

Assessment of mitochondrial content

ASM cells were incubated in complete DMEM media with VEH or with 1 μM AAL-R for 24 h. DNA was extracted using the Qiaamp DNA mini kit (Qiagen, Toronto, ON, Canada) following manufacturer's instructions. Relative expression of mitochondrial DNA (tRNA-Leu(UUR) on nuclear DNA (β2-microglobulin, NC_000015.10) (2) was assessed using SsoAdvanced SYBR Green Supermix kit (Biorad, Hercules, CA). Both primer sets were validated and optimized using standard curves with efficiencies of 100% and 99%, respectively. Melting curves were used to ensure the specificity of the PCR products. Relative quantification of mitochondrial DNA over nuclear DNA was calculated according to Pfaffl (3) and values were reported relative to VEH.

Assessment of mitochondrial activity

ASM cells were incubated in complete DMEM media with VEH or with 1 μM AAL-R for 24 h, trypsinized, centrifuged and resuspended (0.2 million cells per ml) in the Oroboros apparatus at 37°C in complete DMEM. Cellular routine respiration is supported by exogenous substrates in culture media. Routine respiration includes oxygen consumption due to ATP synthesis (phosphorylating state or state 3, OXPHOS) and to proton leak (non-phosphorylating state or state 4). Following stabilization of routine, ATP synthesis was inhibited by oligomycin (2.5 μM) to obtain state 4. State 3 was obtained by subtracting oxygen consumption in state 4 from routine respiration. The maximal

AJRCMB Articles in Press. Published on 27-June-2019 as 10.1165/rcmb.2018-0397OC

activity of the mitochondrial respiratory chain was assessed by titration with the uncoupling protonophore, carbonyl cyanide m-chlorophenylhydrazone factor (CCCP; 0.5 μM in 1 μl/bolus, which transport protons thought the inner mitochondrial membrane). Finally, the activity of complex 3 was blocked with antimycin A (2.5 μM) to measure non-mitochondrial respiration.

Supplemental figure

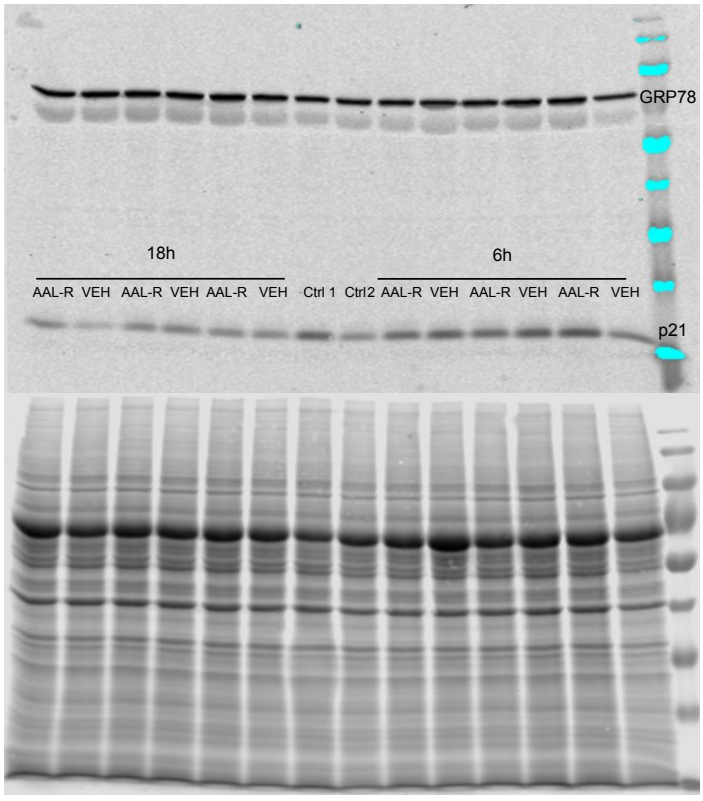

Figure E1. AAL-R does not affect p21 levels. Primary human ASM cells were incubated for 6h or 18h with vehicle (VEH) or AAL-R (1 μM) in complete medium containing 10% FBS. Expression of p21 was assessed by western blot. Shown are complete membrane (top) and REVERT total protein stained blot (bottom) used to generate Figure 2F. The two different Ctrl samples are systematically loaded in all of our gels as quality controls.

References

1. Bosse Y, Thompson C, Stankova J, Rola-Pleszczynski M. Fibroblast growth factor 2 and transforming growth factor beta1 synergism in human bronchial smooth muscle cell proliferation. *Am J Respir Cell Mol Biol* 2006; 34: 746-753.

2. Rooney JP, Ryde IT, Sanders LH, Howlett EH, Colton MD, Germ KE, Mayer GD, Greenamyre JT, Meyer JN. PCR based determination of mitochondrial DNA copy number in multiple species. *Methods Mol Biol* 2015; 1241: 23-38.

3. Pfaffl MW. A new mathematical model for relative quantification in real-time RT-PCR. *Nucleic Acids Res* 2001; 29: e45.